Cerebral Cortex, January 2019;29: 27–41

doi: 10.1093/cercor/bhx301
Advance Access Publication Date: 9 November 2017
Original Article

ORIGINAL ARTICLE

Characteristic Increases in EEG Connectivity Correlate With Changes of Structural MRI in Amyotrophic Lateral Sclerosis

Bahman Nasseroleslami[1], Stefan Dukic[1], Michael Broderick[1], Kieran Mohr[1], Christina Schuster[1], Brighid Gavin[1], Russell McLaughlin[1,2], Mark Heverin[1], Alice Vajda[1], Parameswaran M. Iyer[1], Niall Pender[1,3], Peter Bede[1,3], Edmund C. Lalor[4,5,6,†] and Orla Hardiman[1,3,4,†]

[1]Academic Unit of Neurology, Trinity Biomedical Sciences Institute, Trinity College Dublin, the University of Dublin, 152-160 Pearse Street, Dublin D02 R590, Ireland, [2]Smurfit Institute of Genetics, Trinity College Dublin, the University of Dublin, College Street, Dublin D02 W272, Ireland, [3]Beaumont Hospital, Beaumont Road, Dublin D09 V2N0, Ireland, [4]Trinity College Institute of Neuroscience, Trinity College Dublin, the University of Dublin, Lloyd Building, College Green, Dublin D02 PN40, Ireland, [5]Trinity Centre for Bioengineering, Trinity College Dublin, the University of Dublin, Trinity Biomedical Sciences Institute, 152-160 Pearse Street, Dublin D02 R590, Ireland and [6]Department of Biomedical Engineering and Department of Neuroscience, University of Rochester, Rochester, NY 14627, USA

Address correspondence to Bahman Nasseroleslami, Room 5.43, Trinity Biomedical Sciences Institute, 152-160 Pearse Street, Dublin D02 R590, Ireland. Email: nasserob@tcd.ie, nasseroleslami@gmail.com.

[†]Joint Senior Author.

Abstract

Amyotrophic lateral sclerosis (ALS) is a terminal progressive adult-onset neurodegeneration of the motor system. Although originally considered a pure motor degeneration, there is increasing evidence of disease heterogeneity with varying degrees of extra-motor involvement. How the combined motor and nonmotor degeneration occurs in the context of broader disruption in neural communication across brain networks has not been well characterized. Here, we have performed high-density crossectional and longitudinal resting-state electroencephalography (EEG) recordings on 100 ALS patients and 34 matched controls, and have identified characteristic patterns of altered EEG connectivity that have persisted in longitudinal analyses. These include strongly increased EEG coherence between parietal–frontal scalp regions (in γ-band) and between bilateral regions over motor areas (in θ-band). Correlation with structural MRI from the same patients shows that disease-specific structural degeneration in motor areas and corticospinal tracts parallels a decrease in neural activity over scalp motor areas, while the EEG over the scalp regions associated with less extensively involved extra-motor regions on MRI exhibit significantly increased neural communication. Our findings demonstrate that EEG-based connectivity mapping can provide novel insights into progressive network decline in ALS. These data pave the way for development of validated cost-effective spectral EEG-based biomarkers that parallel changes in structural imaging.

Key words: amyotrophic lateral sclerosis, coherence, electroencephalography, neural connectivity, structural MRI

Introduction

Amyotrophic lateral sclerosis (ALS) is a heterogeneous neurodegenerative disease characterized primarily by degeneration of upper and lower motor neurons (Hardiman et al. 2011) with variable degrees of extra motor involvement. Clinical manifestations of ALS dichotomize into those associated with apparently pure motor system degeneration involving disruption in motor cortex, corticospinal tracts, and motor networks (Bede and Hardiman 2014; Schuster et al. 2016); and degeneration of extra-motor regions, associated with clinical features of cognitive decline, ranging from mild executive impairment through to behavioral variant frontotemporal dementia (bvFTD) (Byrne et al. 2013; Elamin et al. 2017).

While there is an urgent need for noninvasive biomarkers that address disease heterogeneity, the majority of imaging (Bede and Hardiman 2014) and electrophysiological (de Carvalho et al. 2005) studies to date have focussed primarily on quantification of the selective structural degeneration and functional deficiencies of motor pathways. The increasing involvement of broader motor and nonmotor regions and networks suggests that a more extensive assessment of large-scale brain connectivity is indicated.

Previous electro-/magneto-encephalography (EEG/MEG) and functional MRI (fMRI) studies have reported abnormal functional connectivity patterns in neuropsychiatric diseases (Langheim et al. 2006; Georgopoulos et al. 2007), Alzheimer's disease (Stam et al. 2006; Vecchio et al. 2012), Parkinson's disease (Stoffers et al. 2008), and FTD (Pievani et al. 2011). In ALS, fMRI shows increased functional connectivity in the left motor cortex of ALS patients (Agosta et al. 2011) and a previous EEG study has reported increased parietal-to-frontal connectivity (Blain-Moraes et al. 2013). These changes in connectivity have been confirmed by our group (Iyer et al. 2015) in a small sample size ($n = 18$) of ALS patients. We have shown that graph-theoretic measures of connectivity (e.g., degree values, clustering coefficient and assortativity) demonstrate increased connectivity in the θ (central and frontal) and in α and γ bands (widespread). Notwithstanding these findings, the nature of ALS-specific alteration in cortical connectivity (e.g., the brain regions and frequency bands) has not been fully evaluated in the context of disease heterogeneity with broader motor and extra-motor involvement (Hardiman et al. 2011; Al-Chalabi et al. 2016), and the extent by which connectivity changes persist or evolve as the disease progresses is not known. Furthermore, the underlying reasons for disease-specific changes are unclear, and it remains to be determined whether such alterations in connectivity are due to local structural degeneration in motor regions, widespread structural decline, or compensatory neural communication. Resolution of these challenges will provide translational opportunities in ALS whereby the diagnosis, subphenotyping and targeted therapeutics can be based on the underlying changes in specific neural networks.

In this study, we have used high-density EEG to investigate the altered cortical connectivity patterns in a large ALS cohort (comprising 100 patients including 78 spinal-onset, 15 bulbar-onset, and 7 ALS–FTD, including 12 probands carrying the pathogenic hexanucleotide repeat expansion in *C9ORF72*) and 8 patients with bvFTD who had no clinical evidence of motor degeneration. Overall, 34 healthy age-matched controls were included in the study for comparative purposes.

We have identified disease-specific patterns that are significantly different in resting-state recordings between ALS patients and controls. These changes persist on repeated longitudinal assessment, and correlate with structural and diffusion tensor imaging (DTI) MRI measurements from the same patients. Our findings, that the effects of focal disease-specific and broader structural degeneration can be reproducibly characterized using spectral EEG, provide an exciting prospect for the development of novel noninvasive biomarkers in ALS and related neurodegenerative conditions.

Materials and Methods

Ethical Approval

This study was approved by the ethics committee of Beaumont Hospital, Dublin, Ireland (REC reference: 13/102) and the Tallaght Hospital/St. James's Hospital Joint Research Ethics Committee (REC) (REC reference: 2014 Chairman's Action 7, CRFSJ 0046) for St. James's Hospital, Dublin, Ireland. The experimental procedure conformed with the Declaration of Helsinki. All participants, including the patients and healthy controls, provided written informed consent before taking part in the experiments.

Experimental Design

The study sought to find spectral power and connectivity signatures that distinguish ALS patients from healthy controls, using EEG recordings from both groups. No randomization or blinding was applied, as the potential differences between the groups were not known and could not affect the experiment and data acquisition. Power analysis was performed post hoc.

Participants

Patient Recruitment

Recruitment was undertaken from ALS patients attending the National ALS specialty clinic in Beaumont Hospital. Healthy controls were recruited from neurologically normal spouses of ALS patients, and from neurologically normal age-matched individuals recruited as part of an existing cohort study of cognition in ALS.

Inclusion Criteria

The recruited patients, included individuals above 18 years of age diagnosed with ALS, ALS–FTD, or FTD. In the ALS and ALS–FTD groups, patients were within the first 18 months since diagnosis and fulfilled the El Escorial diagnostic criteria for Possible, Probable, or Definite ALS. In the FTD group, patients (including behavioral variant, semantic dementia and progressive aphasia) who fulfilled the revised diagnostic criteria for FTD (Rascovsky et al. 2011) were included.

Exclusion Criteria

Patients diagnosed with primary lateral sclerosis (PLS), progressive muscular atrophy (PMA), flail arm/leg, transient ischemic attack (TIA), multiple sclerosis (MS), stroke, epilepsy, seizure disorder, brain tumors, structural brain diseases, other degenerative brain diseases, and other comorbidities (e.g., human immunodeficiency virus) were excluded.

Demographics of Patients and Controls

A total of 100 patients with ALS (f/m: 30/70; age: 60.2 ± 11.1 years in the range 29–82), 8 patients with FTD (f/m: 5/3; age 66.8 ± 8.1 in the range 57–81), and 34 healthy controls (f/m: 19/15; age: 58.1 ± 13.9 in the range 30–78) were recruited (Table 1). The FTD patients were recruited as part of a parallel study on FTD and the subsequent data analysis for the FTD group was performed separately from the ALS group.

Medical Profile

Within the ALS group (excluding ALS–FTD patients), 78 patients had spinal onset, 15 bulbar onset, and 7 ALS–FTD (4 spinal onset and 3 bulbar onset), as listed in Table 1. For 93 patients, the Revised ALS Functional Rating Scale, ALSFRS-R (Cedarbaum et al. 1999), was carried out ±1 month of EEG data acquisition (not biased to before or after recording, $P > 0.1$, Wilcoxon's Signed Rank test, $n = 100$) and ranged from 13 to 48, with a mean (±SD) of 36.0 ± 7.8 (Table 1). Twelve of 83 patients tested for hexanucleotide repeat expansion in *C9ORF72* had positive results (Table 1). From 93 patients with available family history, 18 had a known family history of at least one first or second degree relative with ALS (Byrne et al. 2012). From 95 patients with known history of taking Riluzole at the time of EEG recording, 12 patients were off Riluzole and 83 were on Riluzole with 69.0 ± 63.0 days (median ± IQR) past since starting the medication.

Experiment

Experimental Paradigm

The experimental paradigm was resting-state with the eyes open, which was undertaken in 3 blocks of 2 min for both the patient and control groups. Subjects sat in a comfortable chair and were required to fixate at the letter X (6 cm × 8 cm) on an A4-sized piece of paper, which was located at a distance of about 1 m in front of them. They were asked to be relaxed and minimize unnecessary eye movements during the EEG acquisition.

Data Acquisition

EEG recordings were conducted in dedicated laboratories in the University of Dublin and St. James's Hospital, Dublin using a BioSemi ActiveTwo system with 128 active sintered Ag-AgCl electrodes and headcaps (BioSemi B.V., Amsterdam, The Netherlands). For spectral power, the 18 recordings performed in hospital were significantly lower (Mann–Whitney *U*-test, $P = 0.0055$, AUC = 0.72, $n_1 = 18$, $n_2 = 82$), therefore, these recordings were excluded from the comparisons of spectral power. Each subject was fitted with an appropriately sized EEG cap. The EEG data were filtered online over the range 0–134 Hz, and digitized at 512 Hz. Longitudinal study, included 4 subsequent recording sessions (T2–T5) scheduled every 4 months after the first recording session (T1), in which 57, 36, 25, and 17 subjects attended, respectively.

Data Analysis

EEG Preprocessing

After the quality checks by visual inspection (EyeBallGUI) (Mohr et al. 2017), we used an automatic artifact rejection method (Dukic et al. 2017) based on statistical thresholding (Nolan et al. 2010) and verified the efficacy of the procedure by visuall inspection in 16 subjects. See the Supplementary Material for details.

EEG Signal Processing

Bipolar channels ($n = 125$) were formed by subtracting adjacent electrodes to estimate the superficial cortical brain activity and minimize the effects of volume conduction and deeper brain sources, as well as to reduce the effects of unrejected artifacts such as EMG (Muthukumaraswamy 2013). The EEG signals were high-pass filtered with cut-off frequency of 1 Hz. To calculate the spectral power, coherency function and coherence (Halliday et al. 1995), the signal was epoched into 1 s segments and multiplied by a Hann window function and then the auto- and cross-spectra were estimated by taking the median of complex frequency domain values across all the data epochs (Dukic et al. 2017). The epoch length did not have a significant effect on results as the findings with 10 s epochs were the same. The band-specific real, imaginary and absolute values of the coherency function were estimated in the δ (2–4 Hz), θ (5–7 Hz), α (α_l: 8–10 Hz, α_h: 11–13 Hz), β (β_l: 14–20 Hz, β_h: 21–30 Hz), and γ (γ_l: 31–47 Hz, γ_h: 53–97 Hz) frequency bands between all 125 bipolar channel combinations (performed in sensor space). These frequency bands were selected according to the frequency ranges that change in motor tasks (Pfurtscheller and Silva 1999; Nasseroleslami et al. 2011, 2014; Vuckovic et al. 2015), as well as resting-state studies in ALS (Iyer et al. 2015) and in healthy subjects (Muthuraman et al. 2015). All the signal analysis was performed in MATLAB (Mathworks Inc., Natick, MA, USA), using scripts coded for this study (See the Supplementary Material for details).

Measures of Spectral Power and Connectivity

The log-scale spectral power, $\log_{10}(1 + F_{xx}(f))$, where $F_{xx}(f)$ represents the auto-spectrum of the signal $x(t)$ at frequency, f, was calculated for each bipolar channel in each frequency band as a measure of spectral power. The real and absolute values of the complex coherency function $C_{xy}(f) = F_{xy}(f)/\sqrt{F_{xx}(f)F_{yy}(f)}$ (where $F_{xx}(f)$ and $F_{yy}(f)$ are the auto-spectra and $F_{xy}(f)$ the cross-spectrum of the signals $x(t)$ and $y(t)$ pertaining to 2 bipolar EEG channels), were calculated for all channel pairs, in each frequency band. For each electrode, the median of the real coherence quantified the oscillation synchrony (real coherence corresponds to zero-lag no-delay synchrony), and the median absolute coherence quantified the (average) connectivity of the node (with arbitrary phase differences); which were calculated

Table 1. Age, gender, diagnosis status and ALSFR-R of the participants

Group	*n*	Male	Female	Age (y)[b]	Dx–EEG T1[a] (days)[b]	ALSFRS-R
Control	34	15	19	58.1 ± 13.9		–
ALS						
All	100	70	30	60.2 ± 11.1	283 ± 357	36.0 ± 7.8 $^{(n=93)}$
Spinal[c]	78	57	21	59.8 ± 11.2	292 ± 379	35.8 ± 7.1 $^{(n=72)}$
Bulbar[c]	15	9	6	57.1 ± 9.6	234 ± 262	35.4 ± 11.1 $^{(n=14)}$
ALS–FTD	7	4	3	71.5 ± 6.9	289 ± 301	38.9 ± 7.1 $^{(n=7)}$
C9ORF72+	12	5	7	60.9 ± 8.6	366 ± 313	37.9 ± 8.8 $^{(n=11)}$
C9ORF72–	71	55	16	61.3 ± 11.5	298 ± 395	35.2 ± 8.0 $^{(n=68)}$
FTD	8	3	5	66.8 ± 8.1	–	–

[a]Dx–EEG T1 is the time interval between diagnosis and the T1 EEG recording.
[b]Numbers show mean ± standard deviation.
[c]The spinal and bulbar groups exclude ALS–FTD patients.

between each node and all other 124 bipolar channels. The average connectivity or synchrony at each electrode was represented by median coherence with all other electrodes, as the change in the value of the median can indicate the overall shift of the group of coherence values. As prewhitening the EEG signals (Georgopoulos et al. 2007) had negligible effect on the results, it was not used for the final analysis. These spectral power, synchrony and connectivity measures were analyzed as groups of multivariate variables. Additionally, to perform univariate statistics, each measure of spectral power and connectivity was averaged across all bipolar electrodes and additionally assessed in ALS patients versus controls. (For verification and validation of these connectivity measures, please see the Supplementary Material.)

Point-to-Point Analysis of Connectivity

The potential point-to-point pattern of the altered connectivity was assessed using 2 approaches. First, the changes in the average connectivity were further inspected by choosing reference or "seeding points." Second, we found the discriminant eigen-connectivities (Leonardi et al. 2013) to extract more explicitly point-to-point patterns (see Supplementary Material).

Linear Discriminant Analysis

Fisher's linear discriminant analysis (Fukunaga 1990; Izenman 2008) (LDA) was applied separately on the 4 EEG and 9 MRI measures to find the most discriminant linear combination of measures based on the eigenvectors of $S_w^{-1}S^b$ (S_b and S_w: between-group and within-group covariance matrices). Additionally, a regularized ($\lambda = 0.05$) LDA was performed on high-dimensional EEG measures (8 frequency bands × 3 measures [power, connectivity, synchrony] × 125 channels = 3000 variables). For EEG measures (but not for MRI), the first discriminant component was the dominant (accounting for more than 90% of discriminatory variance).

Correlates With MRI Scores

Overall, 59 of the spinal- and bulbar-onset ALS patients (including 5 *C9ORF72+* and 38 *C9ORF72−* patients) participated in a parallel MRI study (Schuster et al. 2016), as described in the Supplementary Material. We sought to include measures that were maximally different between the controls and patients (Bede and Hardiman 2014; Bede et al. 2016; Schuster et al. 2016) and to find potential relations between the alterations in EEG and affected regions as defined by MRI. We have previously shown that in spinal onset ALS there is a predominant involvement of posterior internal capsule and medial corona radiata pathology, and that the main motor-related degeneration is the selective involvement of corticospinal and corticobulbar fibers (Schuster et al. 2016). We also included regions (primarily white matter tracts) that are found to contribute to generation of EEG oscillations (Pfurtscheller and Silva 1999; Vuckovic et al. 2014; Xu et al. 2014). Consequently, 9 structural and DTI measures were chosen for correlation analyses on this basis in advance (a priori) of the analysis: Grey matter thickness in the left and right motor areas (separately averaged across precentral gyrus, central sulcus, and superior precentral sulcus), average fractional anisotropy (FA) of the left and right thalamocortical pathways, average FA of the left and right superior corona radiata, average FA of the left and right corticospinal tracts in the internal capsules and cerebral peduncles, and average FA of corpus callosum. These regions were defined by atlas-based segmentation, and were selected due to their known degeneration in ALS (Schuster et al. 2016), or their potential contribution to oscillatory EEG signatures—for thalamocortical projections (Pfurtscheller and Silva 1999). As there was a high level of correlation between these 9 MRI measures of degeneration, Principal Component Analysis, PCA (Jolliffe 2002), was used to extract the principal directions of neurodegeneration, as "degeneration modes." Before PCA, the MRI and EEG scores were transformed to standard normal distributions (see Supplementary Material). The scores corresponding to each degeneration mode were then correlated with measures of spectral power, synchrony and connectivity. As a control, the age-dependent degeneration (found by the correlation vector of the patients' age with structural MRI scores in each mode) was calculated and the percent variance of each degeneration mode explained by age was found. As limiting the analyses to the *C9ORF72−* patients showed negligible confounding effect of the *C9ORF72* genotype on imaging measures (Bede et al. 2013), the MRI–EEG analyses were performed on the entire cohort of 59 patients.

Statistical Analysis

For statistical analysis, we first used frequentist statistics to discard the unaffected measures and to find the potentially interesting effects due to ALS; next, we used Empirical Bayesian inference (EBI) to more accurately infer the disease-specific effects in the presence of complex high-dimensional correlations in the data (difficult to address with frequentist methods), but more importantly to estimate the statistical power and Bayesian posterior probabilities.

Frequentist Statistics

The between-group comparisons of spectral power and connectivity measures were performed using the *P*-values of the Mann–Whitey *U*-test and the area under the curve (AUC) for the receiver operating characteristic (ROC) curve (Zhou et al. 2009). The pairwise comparisons (e.g., for longitudinal data) were performed using Wilcoxon's Signed Rank test. For comparison of several groups (ASL phenotypes), the Kruskal–Wallis nonparametric 1-way analysis of variance test was employed. Analysis of correlations was performed using Spearman's rank correlation coefficients. The frequency measures were assessed within the 8 defined frequency bands. To account for multiple comparisons, rejection of null hypotheses was performed by adaptive false discovery rate (aFDR) at $q = 0.05$ (Benjamini and Hochberg 1995; Benjamini et al. 2006). For each measure and frequency-band, the FDR was applied on the bipolar channels being compared ($n = 125$), that is, across channels but not across measures or frequency bands. This procedure served as a screening method for potentially significant differences between the groups. A similar procedure was used to assess the significance of individual connections when seeding from one channel at a specific frequency band at $q = 0.10$.

To assess the statistical significance of the eigenvectors from PCA and LDA for EEG and MRI measures, a null and non-null bootstrapping resampling approach was used to calculate the standard deviations, *P*-values and statistical power (see Supplementary Material).

Empirical Bayesian Inference

EBI (Efron et al. 2001; Efron 2007) is a statistical approach for inferring statistical significance and finding effects in individual variables of high-dimensional observations. It uses a test statistic in each variable to quantify the level of effect in/between the groups. The test statistic values for all variables using the

original observations, as well as the null-permuted data are used to estimate the probability density function of the data and the null, respectively. Subsequently, the prior and posterior probabilities are estimated from the density functions; which are used to estimate the FDR and statistical power for each threshold level of the posterior probabilities. The EBI was applied on the AUC for the ROC curve (Zhou et al. 2009) as the test statistic, for statistical analysis of the spectral power and connectivity measures between ALS and controls. For each measure, data from the 8 frequency bands and 125 bipolar channels were analyzed together (1000 variables).

Results

Analysis of differences in neural activity and connectivity between the ALS cohort and controls in the characteristic EEG frequency bands showed significant differences after aFDR corrections (Supplementary Figures S2–S4). Additional analyses based on the statistical power and Bayesian posterior probabilities further confirmed the findings (Supplementary Figures S2 and S3, rows 4).

Decreased Spectral Power

We detected a significant decrease in the low-frequency (θ-band) spectral power in ALS patients (excluding pure FTD patients) versus healthy controls (Fig. 1). This decrease of θ-band power in ALS patients was significant over bilateral motor areas of scalp, and spread to other scalp locations and the adjacent frequency bands (δ- and α_l-bands) (Supplementary Figure S2).

Increased Average Connectivity

We detected widespread and significant increases in average connectivity in ALS patients compared with healthy controls (Fig. 1). The most notable changes were detected over bilateral motor regions of scalp for θ-band and over parietal and frontal scalp regions for γ-band (Supplementary Figure S3). This strong effect also spread to adjacent locations and frequency bands.

Alterations in average synchronous EEG oscillations were also captured (Supplementary Fig S4). In ALS patients, the γ-band average synchrony was significantly reduced above bilateral primary motor areas of scalp (with additional but lesser involvement of parietal–occipital scalp regions), suggesting that altered neural activity in motor cortical areas was a function of structural change.

The identified increases in the average connectivity were further inspected to determine whether they originated from specific increases in point-to-point connectivity. For this purpose, overall connectivity across regions was inspected in the corresponding frequency bands. The lateral-central C_4 and midline-parietal P_z channels (representing bilateral motor, and parietal scalp regions) were chosen as reference or "seeding points" (Fig. 2), as these regions showed significant ALS-specific changes in the average connectivity. This analysis showed that increased connectivity in the θ frequency band originated from increased connectivity between left and right motor areas of scalp (Fig. 2). Similarly, increased connections in γ frequency band were found within parietal scalp areas and between parietal–frontal scalp regions.

Analysis of changes in the point-to-point connectivity (without reference to average connectivity) also showed significant differences between controls and ALS patient group (Supplementary Figure S5). The major effects were the increased coherence in θ-band between the scalp regions over the 2 motor areas, and pattern of the increased coherence in γ-band between the parietal–frontal scalp regions. The main eigen-connectivities (Fig. 2, bottom row) show the dominance of these patterns more explicitly.

These 4 spectral power and connectivity measures that showed significant changes in ALS (θ-band spectral power, θ-band connectivity, γ-band connectivity, and γ-band synchrony), were used as 4 average (across all electrodes) measures to further study the changes in the ALS group.

ALS can be Discriminated From Controls Using Spectral EEG Based Mapping

A comparison between ALS and controls was performed in individual channels (topographic maps), as well as on average across all bipolar electrodes in the affected frequency bands using the linear discrimination combination of 4 spectral power and connectivity measures (Fig. 3). The findings closely resembled the individual patterns of change in both average quantitative measures and topographic maps, confirming that the detected changes are not only valid detections, but also key discriminants between ALS and controls.

EEG Differences Between ALS Patients and Controls do not Discriminate Between ALS Subgroups

Connectivity measures that discriminated between ALS patients and controls were used to measure differences between traditionally-defined ALS subgroups (bulbar onset, spinal onset, ALS–FTD, FTD, and the presence or absence of the *C9ORF72* variant) (Fig. 4). While these measures were different between ALS and controls, there was no difference between ALS subgroups (Supplementary Figure S6), although increased parietal–frontal connectivity was strongly present in FTD patients without ALS, and the median γ_h connectivity measure (Fig. 4) was significantly higher for FTD compared with the control group (Mann–Whitney *U*-test, $P = 0.0073$, AUC = 0.83, $1–\beta_{0.05} = 0.87$, $n_1 = 34$, $n_2 = 8$) but was not higher than the ALS group.

Degeneration in Structural MRI Shows Discriminatory Power Comparable to EEG Features, but With a Complex Pattern

To validate the findings of altered connectivity as markers of selective networks disruption, we sought to determine the relationship of our observed neurophysiologic signatures with ALS-specific MRI changes in 59 ALS patients who had undergone contemporaneous scans (Bede et al. 2016; Schuster et al. 2016). The focus was on 9 regions of interests (including both grey and white matter) that show maximal degeneration and/or contribute to EEG oscillations which were selected from MRI data. The AUC values for these MRI measures (Fig. 5, top) were comparable to the EEG measures (Fig. 3, top) in terms of discriminatory power. The maximally discriminant MRI (Cortico-Spinal Tract's FA) and EEG (γ-band median connectivity) measures had similar AUC of 0.73, while the average of the AUC values for the 4 EEG measures (0.69) was higher than the ones for 9 MRI measures (0.66). See Table S1.

Linear discriminant components are shown in Figure 5. While all of the MRI measures decreased in ALS, the discriminant components were not symmetric. We found that the discriminant vectors did not resemble the average changes in MRI individual measures (Fig. 5, top). Rather, the average changes in MRI measures were due to the combined effect of several subcomponents (in contrast to the EEG where the main discriminant

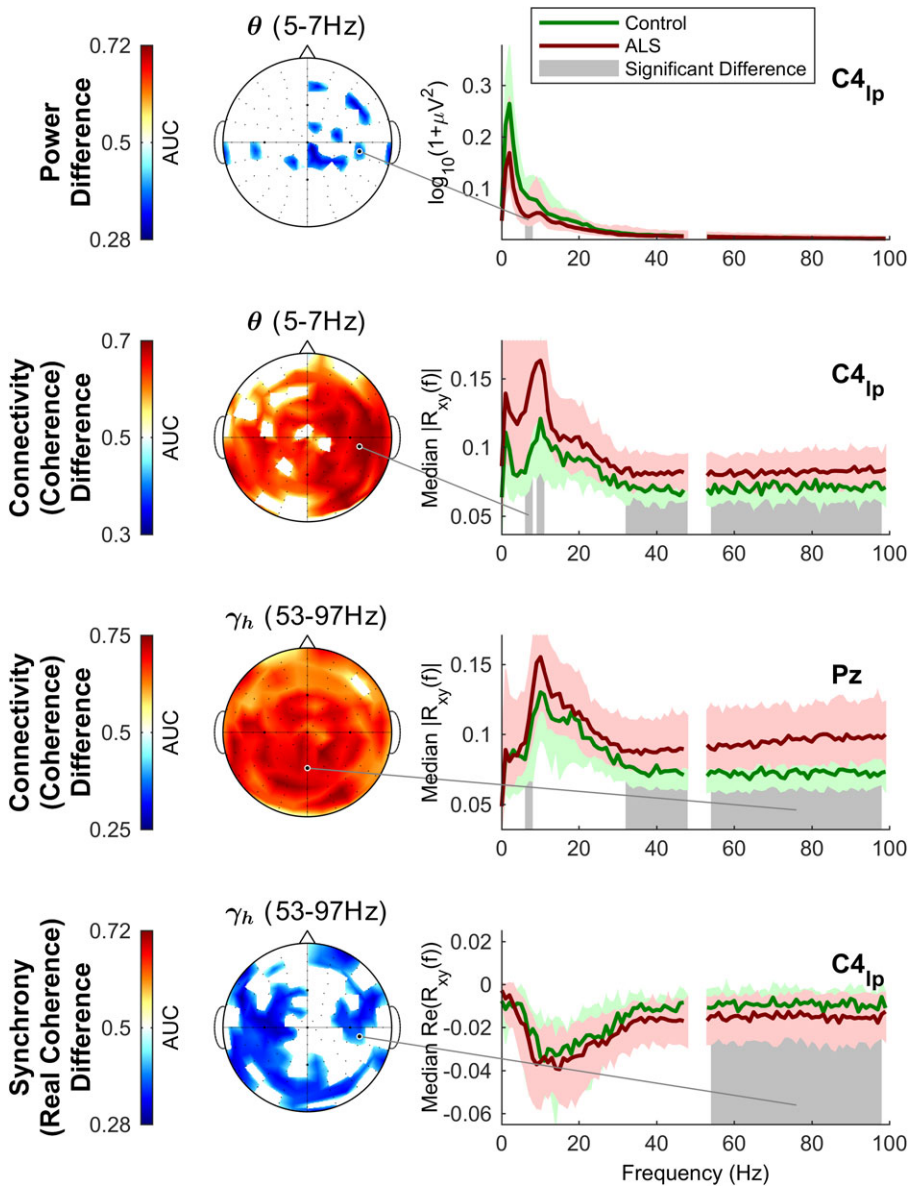

Figure 1. In ALS patients, spectral EEG power is significantly decreased in θ-band over the bilateral motor regions of scalp, while the median coherence is significantly increased in θ-band over motor areas and in γ-band over parietal and frontal scalp regions. The spectral power and median coherence are shown in 2 representative electrodes $C4_{lp}$ (right motor region) and P_z (parietal region) over scalp as a function of frequency. The spatial spread of the altered features is shown topographically in the θ- and γ_h- frequency bands. Significant difference between the healthy controls (n = 34) and ALS patients (n = 100) was assessed in the 8 defined frequency bands using Man–Whitney U-test and adaptive false discovery rate (FDR), as elaborated on in supplementary Figures S2 and S3. Notice the extension of changes to adjacent frequency bands (from γ to β_h). AUC: area under the receiver operating characteristic (ROC) curve.

component resembled the average changes in individual measures). These data suggest that the relationship between MRI changes and EEG changes in ALS is complex (a multiparameter relationship/correlation that cannot be explained by a simple one-to-one relationship). Because it was not possible to infer the overall differences by inspection, we used a combination of PCA and several low and high-dimensional correlations to further study the complex relationship between MRI and EEG findings.

Changes in EEG Power and Coherence Correlate With Changes in Structural MRI Measures

As there was a high level of correlation between the MRI indices, PCA was used to extract the principal modes of neurodegeneration. The scores corresponding to each degeneration mode were correlated with measures of spectral power, synchrony and connectivity using the spectral EEG datasets, while recognizing that the MRI degeneration modes were combinations of changes in both grey and white matter.

The PCA-extracted modes of degeneration included 3 principal components that accounted for 57.3%, 20.4%, and 8.4% of normalized variance. The first 3 degeneration modes accounted for variances larger than (or comparable to) those of age and the direction of their eigenvectors were statistically consistent (Fig. 6). The first of these, involved widespread general degeneration in all regions of interest (consistency: P = 0.0001, $\beta_{0.05}$ = 1e-6), which resembled the variability modes in healthy controls and age-related degeneration, albeit accounting for more

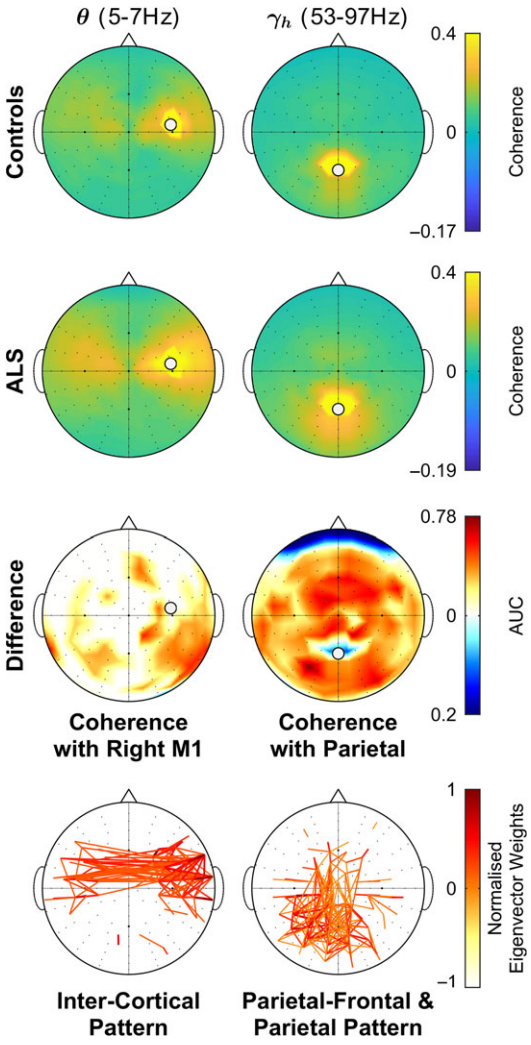

Figure 2. The dominant changes in EEG connectivity include increased θ-band intercortical and γ-band frontoparietal coherence over scalp. The average values in controls and ALS groups, as well as between-group (ALS-Control) differences in coherence is shown with reference to (i.e., taken as connectivity seeds) the areas with dominant change in median connectivity: *Left*: Change in θ-band median coherence over scalp motor areas (see Supplementray Figure S3) expanded by seeding from right M1 (location C_3). Notice the higher connectivity between ○ (right) and the left motor areas over scalp. *Right*: Changes in γ-band median absolute coherence in parietal and frontal scalp areas (see Supplementary Figure S3), expanded by seeding from parietal area (location P_z). Notice the higher connectivity between ○ and both parietal and frontal scalp areas. Only the statistically significant connections (adaptive FDR, $q = 0.1$) are shown. AUC: area under the receiver operating characteristic (ROC) curve. *Bottom row*: Point-to-point connectivity patterns from discriminant eigenconnectivity analysis (see Supplementary Material), confirming the increase in θ-band intercortical and γ-band frontoparietal coherence.

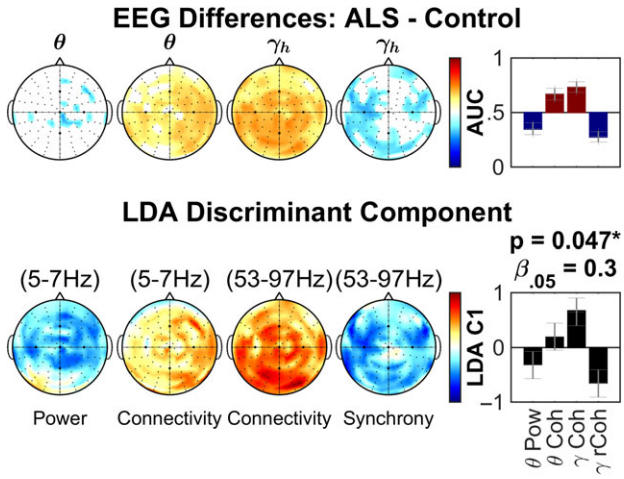

Figure 3. The linear discriminant analysis (LDA) direction for spectral EEG power and connectivity measures is similar to the differences of individual measures between ALS and controls, both for topographic maps and individual measures. The 4 EEG measures include the θ-band spectral power (θ Pow), θ-band median coherence (θ Coh), γ_h-band median coherence (γ Coh), and γ_h-band median real coherence (γ rCoh), all averaged across all electrodes, as in Figure 3. Bar plots (right): The individual measures are compared on top, while the eigenvector of LDA is shown on the bottom. AUC: area under the receiver operating characteristic (ROC) curve. The *P*-value and $\beta_{0.05}$ correspond to the shape (and not the presence of) of the LDA eigenvector. Topographic maps (left): comparison of individual electrodes for each measure between controls and ALS patients is shown on top, while the first eigenvector (LDA C1) of high-dimensional regularized LDA (125 channels × 3 measures × 8 frequency bands = 3000) is shown on the bottom (only 4 × 125 = 500 relevant variables of the vectors are shown in the topographic map). See text for methods and statistics. Error bars: standard deviations.

than 4 times the variance than was explained by age. This mode was correlated with median coherence in θ-band (and in γ-band), as well as the spectral power in θ-band. The overall correlation of the scores of this mode with the EEG scores along the individual EEG–MRI correlation vector was $r = 0.28 \pm 0.096$ ($P = 0.043$, $\beta_{0.05} = 0.25$). The second degeneration mode was formed primarily by the differential degeneration of corticospinal tracts and motor cortex, thus representing a motor-related disease-specific degeneration (consistency: $P = 0.00033$, $\beta_{0.05} = 0.00033$). This emphasized the differential degeneration of white and grey matters in motor cortical regions and tracts. Importantly, this mode was strongly correlated with θ-band spectral power (and γ-band synchrony). The overall correlation with EEG scores along the individual EEG–MRI correlation vector was $r = 0.42 \pm 0.1$ ($P = 0.0094$, $\beta_{0.05} = 0.041$). The third degeneration mode did not show any notable correlations with the EEG measures. The topographic maps of these correlations were similar to the topographic maps of the significant changes in ALS versus controls. (See the Supplementary Material—Figures S7 and S8—for the detailed topographic maps of EEG correlations with MRI scores and the corresponding statistical inference.)

Taken together, these data showed increased connectivity and reduced synchrony and spectral power measures in ALS patients which correlated to the MRI scores of structural neurodegeneration in the regions extensively or moderately affected in ALS (see the correlation data in Fig. 7, top). The scalp regions with increased EEG connectivity extended beyond the regions over motor areas affected in ALS, which is an indication of both direct and indirect effects of neurodegeneration on spectral EEG measures.

Longitudinal Study of EEG Measures Shows Progressive Increase in Connectivity

We examined the longitudinal changes in spectral EEG at 4 subsequent recording sessions (T2–T5) scheduled every 4 months after the initial recording session (T1) for each patient. Significant progressive changes were noted in connectivity, when the average quantitative measures were examined as

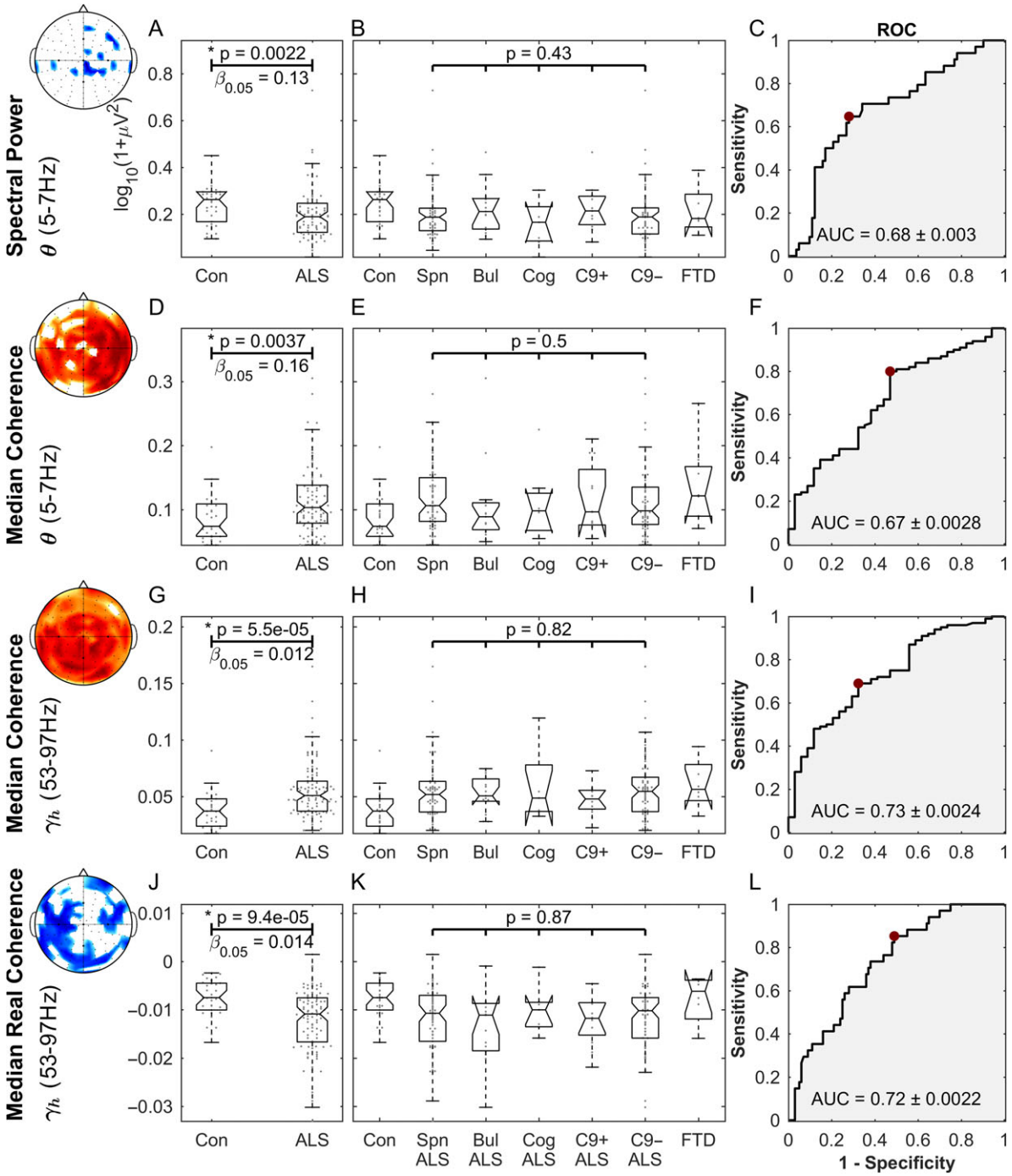

Figure 4. The spectral EEG power and connectivity measures are different between ALS and controls, but not between ALS subgroups. (*A*, *D*, *G*, *J*) Comparison between healthy controls and all ALS patients. (*B*, *E*, *H*, *K*) Comparison between ALS subgroups. "Con", "Spn", "Bul", "Cog", "C9+", and "C9-" stand for Control, Spinal, Bulbar, ALF-FTD, *C9ORF72*-positive, and *C9ORF72*-negative subgroups, respectively. (*C*, *F*, *I*, *L*) Receiver operating characteristic (ROC) curve, comparing the discriminatory power, the optimal level of sensitivity-specificity (red dot), as well as the area under the curve (AUC), achieved for linear discrimination of controls and ALS patients using each measure. For each measure and frequency band, the average of all bipolar electrodes is used. See text for methods and statistics.

univariate measures (Fig. 7). These changes were all consistent in direction as the disease progressed, showing an accentuation of the signatures. However, when the multivariate topographic maps were tested for significant changes (corrected for multiple testing), only the θ- and γ-band coherences exhibited a significant increase in specific scalp locations (Supplementary Figure S9).

Gender, Age, and Medication Effects on EEG Measures

To ensure that the observed effects were not affected by other confounding factors (e.g., the effect of medications including the antiglutamate drug Riluzole) and to evaluate the effect of age, gender, and clinical disability, additional confirmatory tests were performed.

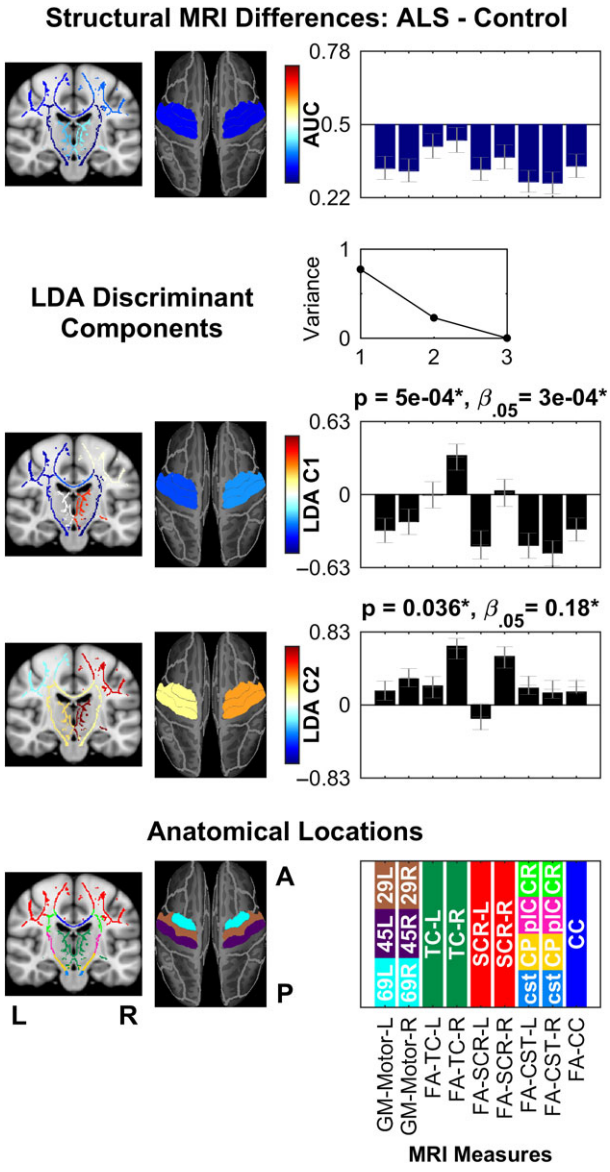

Figure 5. The Linear Discriminant Analysis (LDA) directions for MRI measures are more complex than the differences of individual measures between ALS and controls. The 9 MRI measures include Grey Matter Thickness (Destrieux et al. 2010) in left and right motor cortices (GM-Motor-L and GM-Motor-L), Fractional Anisotropy (Oishi et al. 2008) in left and right Thalamocortical pathways/loops (FA-TC-L and FA-TC-R), Superior Corona Radiata (FA-SCR-L and FA-SCR-R), Corticospinal Tracts (FA-CST-R and FA-CST-R), as well as Corpus Callosum (FA-CC). See Schuster et al. (2016) and the original references (Oishi et al. 2008; Destrieux et al. 2010) for the details. Bar plots (right): The individual measures are compared on top, while the eigenvectors of LDA are shown in the middle. AUC: area under the receiver operating characteristic (ROC) curve. The P-value and $\beta_{0.05}$ correspond to the shape of the LDA eigenvectors. MRI maps (*left*): Comparison of individual measures between controls and ALS patients is shown on top, while the first and second eigenvectors (LDA C1 and C2) of LDA are shown in the middle. AUC: area under the receiver operating characteristic (ROC) curve. See text for methods and statistics. A/P/L/R: anterior/posterior/left/right. Error bars: standard deviations.

There was no effect of age or gender in the controls for EEG spectral power or connectivity measures. Neither was there any effect of age, gender, or disease-duration in the ALS patients for any of the EEG measures.

More importantly, none of the major EEG indices (as shown in Fig. 4) was different between patients on Riluzole and those not on Riluzole ALS therapy ($P > 0.10$, Mann–Whitney U-test, $n_1 = 83$, $n_2 = 12$). Spearman's rank correlation did not show any significant relationship ($P > 0.1$, $n = 83$) between the EEG measures and the time duration that patients had been on Riluzole at the time of EEG recordings. Similar analysis found no correlations of the EEG measures with time-since-diagnosis or the clinical disability scale (ALSFRS-R scores, sub-scores, nor fine/gross motor factor-scores) (Cedarbaum et al. 1999). Therefore, the identified EEG signatures were not directly related to motor disability, but rather reflected key patterns of disease-specific network alterations.

Finally, potential changes in the peak frequency, a commonly inspected spectral measure, were analyzed. There were no significant shifts in the peak frequency for spectral power or median coherence in any of the 125 EEG channels (Mann–Whitney U-test, $n_1 = 34$, $n_2 = 100$, $n_{\text{comparisons}} = 125$, $q_{\text{FDR}} = 0.1$).

Discussion

Our data demonstrate that high-density spectral EEG mapping is a potentially robust tool in the assessment of selective changes in neural connectivity in ALS. Notably, spectral power (decrease in θ-band over motor scalp areas), oscillation synchrony (decrease in median real coherence in γ-band) and functional connectivity (higher median coherence in θ-band between bilateral scalp regions over motor areas, and in γ-bands between parietal and frontal scalp regions) are reliable characteristic discriminating factors between ALS patients and healthy controls. Furthermore, changes in spectral power and EEG coherence correlate with structural changes in key brain regions (Fig. 6). Our findings therefore point to a novel, network-wise characterization of neurodegeneration in ALS, which is based on altered connectivity patterns with a specific signature of increased θ-band coherence between the motor regions of scalp and increased γ-band parietal–frontal coherence.

These changes are unlikely to originate from artifacts, as the location of electrodes that show maximal connectivity increase are not the expected locations for eye-movement (frontal electrodes) or EMG (peripheral electrodes) artifacts. This was additionally confirmed using ICA preprocessing for further artifact removal (see Supplementary Material). Moreover, the seeding patterns (Figs 2 and S5) show that the patterns of increased connectivity are maximal over 2 scalp regions (parietal and frontal; left and right) and not only in a single large region. Additionally, the increased connectivity due to an increased activity in a focal source (a single neural brain source or an artefactual component), would simultaneously lead to increased spectral power, while we observed unchanged or decreased spectral power in ALS. Furthermore, the phase values for a notable number of coherence values are distant from 0 or $\pm\pi$ (values expected due to point-spread or single artefactual components). Finally, the attempt to map the changes in cross-spectra to focal sources failed, as it led to distributed sources across the brain regions (Supplementary Material). Taken together, the observed increased connectivity is not likely to be due to artifacts or a single deep source. (See also Supplementary Material for the extended methods and results on the verification of the connectivity measures.)

Inference From High-Dimensional Data

Previously, high-dimensional analyses of connectivity patterns have been challenging due to multiple comparison problem and lack of reproducibility, especially for fMRI studies

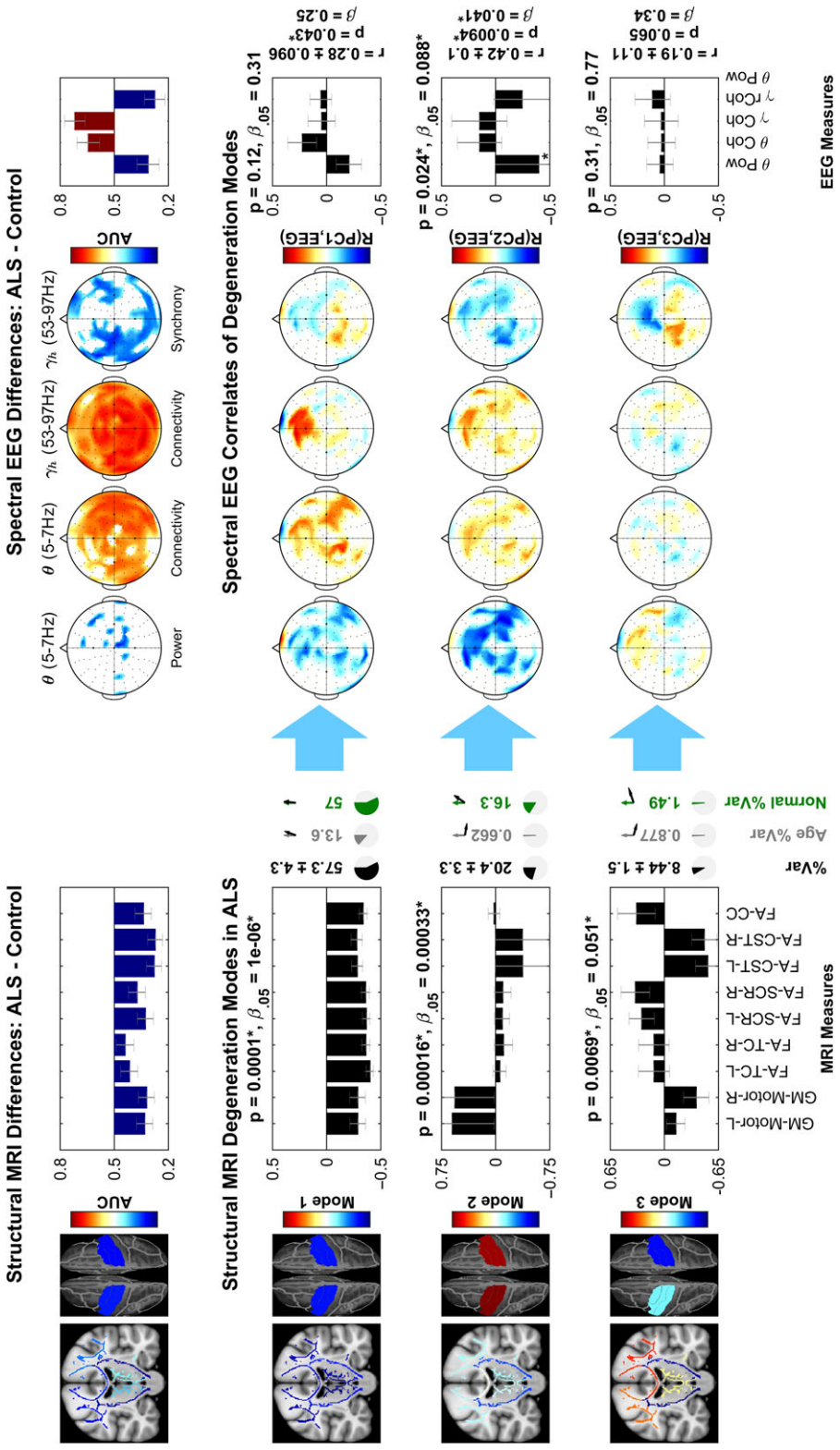

Figure 6. The MRI degeneration mode pertaining to motor-specific decline in ALS is significantly correlated with the decreased spectral power and oscillation synchrony, while the general uniform degeneration mode is additionally correlated with the increased coherence. The top row shows the ALS-specific changes in MRI (left) and EEG (right), side by side (see Figs 4 and 5). Rows 2–4 show the first 3 modes of degeneration in structural MRI found by PCA (left), as well as their correlations with EEG measures (right). The percent of the variance explained by each mode, the parts explained by age, or along the structural covariance modes in healthy controls, as well as the angle of mode's direction with age or normal covariance are shown with black, grey, and green pie plots and vectors. The *P*-value and $\beta_{0.05}$ above the bar plots correspond to the shape of the eigenvectors or degeneration vectors. The error bars and "±" show standard deviations calculated from non-null bootstrapping. "+": Significance at $P < 0.05$, "*": aFDR significance at $q = 0.05$. The *r*, *P*-value, and $\beta_{0.05}$ to the right of correlation vectors correspond to the correlation of the overall EEG measures along the correlation vector direction with MRI.

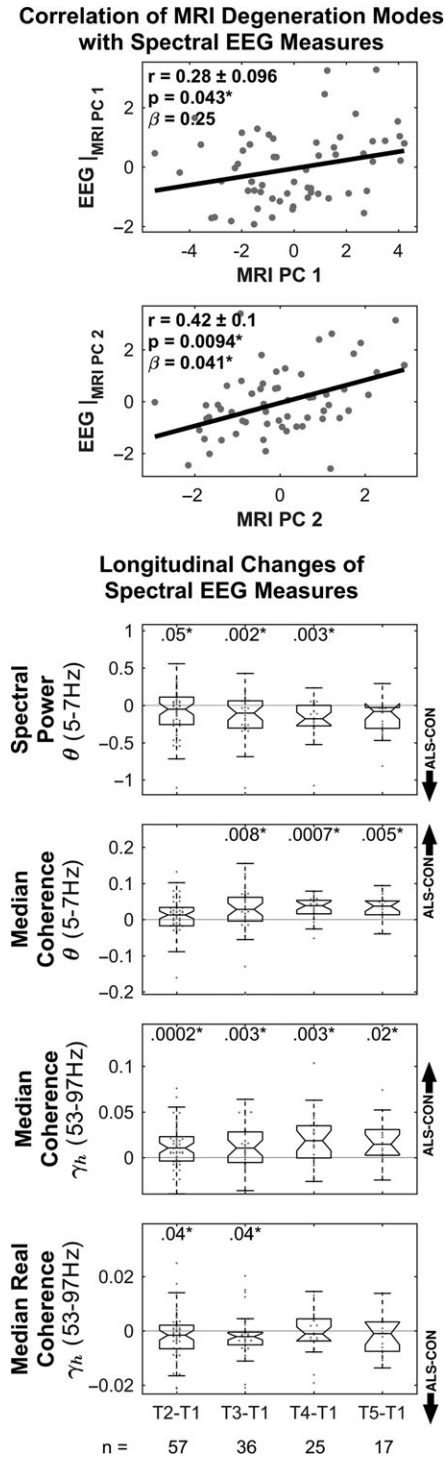

Figure 7. *Top*: The MRI and EEG scores show the correlation of the degeneration modes 1 (general uniform degeneration) and 2 (motor-specific decline) with the altered EEG measures. The scores and the linear regression lines correspond to the rows 2 and 3 in Figure 6. *Bottom*: The Longitudinal spectral EEG power and connectivity measures continue to change in a 16-month follow-up, in the same direction as ALS versus healthy controls. The bar plots show the pairwise differences of the 4 EEG measures (used in Figs 3, 4 and 6) in follow-up sessions T2, T3, T4, and T5 against the first recording T1. The numbers above the boxplots show the aFDR-corrected significant *P*-values of the Wilcoxon's Signed Rank test. The arrows on the right show the direction of change of the measures in ALS (T1) versus healthy controls (Fig. 4).

(Eklund et al. 2016). Our study implemented several approaches to avoid false discoveries. These included a large sample size and the use of a frequentist method (adaptive false discovery rate, aFDR) to limit the false discoveries. We also used EBI to validate the achieved false discovery rate and importantly estimate the Bayesian posterior probability. We estimated statistical power for low-dimensional and high-dimensional data to validate the reproducibility of findings and relied on inference from average values rather than hand-picked measures. The longitudinal follow-up data show similar patterns of changes in the course of the disease and act as retests.

Potential Mechanisms of Changes in EEG

The distinct correlations between MRI metrics and EEG measures indicate the involvement of corresponding structural regions which provides the anatomical substrate of the EEG alterations detected. Specifically, the decreased spectral power in θ-band (and adjacent frequency bands) and the altered γ-band synchrony in bilateral motor regions of scalp are paralleled by structural degeneration in motor cortex and corticospinal tracts in ALS. This interpretation is supported by our data: firstly, both the power and synchrony changes are concentrated above motor regions (about C_3 and C_4 locations) where the disease-specific degeneration is maximal; secondly, the second degeneration mode represents ALS-specific degeneration (including the differential white-grey-matter degeneration) with strong correlation with θ-band spectral power. Finally, although the changes in the spectral power were not as strong as changes in coherences, the spectral power showed a stronger correlation with motor-related disease-specific degeneration.

Segregation of variability in our MRI data into degeneration modes also yielded a widespread pattern of degeneration (resembling the normal covariance in controls) that included areas known to be severely affected in ALS (grey matter motor regions and corticospinal tracts); moderately affected in ALS (superior corona radiata and corpus callosum) and areas that are clinically less apparent (Thalamocortical pathways). EEG correlates of this degeneration mode are a decline in spectral power, with a concomitant increase in functional communication (θ-band intercortical coherence and γ-band parietal–frontal coherence over scalp). These changes can be interpreted based on the existing knowledge on the neuropathology of the condition. In typical ALS, progression is thought to involve initial primary degeneration within the motor system (especially the upper and lower motor neurons) (de Carvalho and Swash 2016; Huynh et al. 2016), with spread to other regions as the disease progresses (Bede et al. 2016; Burke et al. 2017). Therefore, the spectral power decrease in θ-band which is maximal above the motor regions of scalp and maximally correlated with motor-related degeneration modes, mainly reflects the primary motor aspect of the disease. On the other hand, the connectivity increases (especially the γ-band increase between parietal and frontal scalp regions; also strongly present in FTD) that shows considerable longitudinal progression, reflect mostly the spread of the disease to other regions. Further validation of this explanation is warranted in future studies.

In a situation where the baseline neural activity and communication is constant, degeneration in white matter is expected to attenuate communication and connectivity. The observation of increased coherence is therefore likely to reflect extra compensatory activity within and outside areas

associated with white matter degeneration. This change may be a signature of network over-activity and a reflection of the disease severity. Our data therefore indicate that coherence, which quantifies neural communication in the brain, can also indirectly reflect structural degeneration, and can be potentially harnessed to characterize progressive neurodegeneration. Future studies using computational neural modeling would be of utility in assessing this perspective, as invasive neurophysiological recordings in human disease would be precluded by ethical considerations.

The underlying mechanisms for ALS are not yet fully understood and are most likely heterogeneous, (Al-Chalabi and Hardiman 2013). One possibility is that early neurodegeneration of interneurons interrupts the balance between excitatory and inhibitory network activity (Turner and Kiernan 2012). Another possibility is that pathological changes in excito-inhibitory networks are driven by a combination of "dying-forward" and "dying-back" of individual groups of neurons, and that neuronal death occurs as a function of excessive excitotoxicity (Kiernan et al. 2011). There is preliminary evidence for both possibilities, and while the structural neurodegeneration is reflected in the MRI measures and the unbalanced excito-inhibitory network activity reflected in EEG measures, the causality between the changes in the EEG and MRI measures remains to be determined.

In this study, we used the real part of the coherence measure to index frequency-specific synchronous oscillations (i.e., oscillations with zero lag), as has been previously described for the time domain using prewhitened cross-correlations in MEG (Langheim et al. 2006; Georgopoulos et al. 2007). These synchronous oscillations were interpreted as originating from structural neural pathways such as thalamocortical pathways (loops) that lead to simultaneous zero-lag propagation of oscillatory brain activity (Langheim et al. 2006). Consequently, the observed patterns of synchrony alteration (Fig. 3), is an indication of structural separation and isolation of motor cortex from more frontal and parietal regions in the brain. This measure was specifically included as the zero-lag synchronous neural oscillations and has been shown previously to discriminate between healthy individuals and neuropsychiatric patients (Georgopoulos et al. 2007). The utility of this measure was afforded by the bipolar spatial filters applied that attenuate the field-spread effects of deeper sources, hence, allowing the bona fide 0-lag synchrony be aggregated between superficial sources. The correlation with motor-specific degeneration in MRI and concentration over bilateral M1 areas support the validity of this measure.

Utility of EEG for Studying and Diagnosing Neurodegeneration

The observed EEG signatures provide additional and important insights into ALS pathogenesis, which are beyond the scope of current structural MRI and clinical evaluation. Despite the traditional view that ALS is a focal structural degeneration of motor neurons, these data point to major changes that occur at the network level (found by EEG measures of neural activity and connectivity) which correlate in a complex manner with structural degeneration. Furthermore, these changes are related (though through a complex mechanism with direct and indirect effects) to the structural degeneration. The absence of a correlation with clinical phenotypes, while not intuitive, suggests that the patterned changes that we observed in both crossectional and longitudinal datasets are consistent markers of the disease process, regardless of the clinical disability profile. This is an important observation, indicating that spectral EEG has potential for development as a novel biomarker of network degeneration. The correlation with MRI findings, and the progression of observed changes over time support the potential clinical utility of spectral EEG as a disease biomarker, and refinement of these combined measures could form a new basis for novel definition of disease classification (Al-Chalabi et al. 2016). Moreover, this spectral and connectivity-based characterization is also applicable in cognate neurodegenerative diseases, particularly FTD. The increased Frontal-Parietal connectivity changes identified in ALS are also strongly present in the FTD cohort, supporting the notion that it is a neural signature indicative of frontal dysfunction in FTD. Overall, the connectivity-based characterization informs of the altered functions of the network and paves the way for future network-based characterization and mapping of the neurodegenerative diseases.

While the primary goal of this study was to elucidate disease-specific changes and their underlying mechanisms, these measures also have potential as future targets for diagnosis and prognosis of specific aspects of the disease. Our data provide a robust proof of concept for the use of spectral EEG for patient stratification based on network-based pathology in the neurodegenerative disorders. Such an approach has significant advantages over other imaging and diagnostic modalities (e.g., MRI). Given the relative differences between EEG and MRI in terms of cost and accessibility, it is noteworthy that the discriminatory power of EEG coherence measures (based on AUC values) was actually comparable or higher than individual MRI measures (see Table S1). EEG closely reflects the real-time neural activity with excellent temporal resolution, is widely accessible, portable and inexpensive. Spectral EEG recordings can be performed comfortably in extended ranges of patients with neurological impairments within existing clinical settings. The potential diagnostic utility can be further enhanced using previously reported pattern analysis techniques (Georgopoulos et al. 2007; Herman et al. 2008) and/or neuroelectric source imaging (Muthuraman et al. 2014; Lei et al. 2015). Future studies using task-based paradigms, including motor (Fisher et al. 2012) and cognitive tasks (Iyer et al. 2017), carry additional potential in deconstructing sensory or motor aspects of neuropathology, including those that are specifically captured by these resting-state measures.

Limitations

The identified changes in spectral power and connectivity have been assessed in the sensor space corresponding to scalp locations that provide relatively low spatial resolution. Using source analysis (Ramírez et al. 2010; Khan et al. 2015; Muthuraman et al. 2015) to identify the corresponding brain regions that give rise to the reported findings has the potential to further enhance our understanding of the underlying disease pathophysiology in future studies. While challenging and requiring special considerations due to the potential confounding factors of neurodegeneration and the resulting structural changes in the brain, the potential benefits would be considerable.

Additionally, investigation of the effects of mimic disease conditions and other neurological diseases (other than the ALS–FTD range) on the identified EEG signatures will be required to establish the specificity of this technology for adjunct diagnostic purposes.

Conclusions

This is the first study of its kind to demonstrate the validity of spectral EEG as a measure of structural degeneration in ALS. Correlations between EEG measures and contemporaneous changes in structural MRI indicate that changes in neural activity in motor areas mirror focal disease-specific structural changes in ALS. Moreover, the increased connectivity (coherences) reflects network over-activity in affected motor regions (intercortical θ-band) and less degenerated regions such as parietal and frontal areas (γ-band), and likely represents an indirect potentially compensatory effect of degeneration.

Our data confirm that spectral EEG is a novel and potentially sensitive methodology by which the neurodegeneration in ALS and related conditions can be characterized in terms of specific disruptions in neural communication. This technology can be harnessed as an inexpensive and clinically useful disease biomarker in assessing the efficacy of targeted drug therapies for neurodegeneration.

Supplementary Material

Supplementary data is available at *Cerebral Cortex* online.

Funding

Health Research Board of Ireland (award HRA-POR-2013-246); and Irish Research Council (Government of Ireland Postdoctoral Research Fellowship GOIPD/2015/213 to B.N.). The neuroimaging (magnetic resonance imaging) aspects of the study were supported by the Health Research Board of Ireland (Emerging Investigator Award HRB-EIA-2017-019), the Irish Institute of Clinical Neuroscience (IICN) - Novartis Ireland Research Grant, The Iris O'Brien Foundation, and The Perrigo Clinician-Scientist Research Fellowship.

Notes

We would like to thank the students and staff at Trinity Biomedical Sciences Institute, Trinity College Institute of Neuroscience, St. James's Hospital (HRB-Wellcome Trust Clinical Research facility), and Beaumont Hospital who facilitated this study. We would like to thank all the patients and their families who contributed their time for this research. The majority of calculations were performed on the Lonsdale cluster maintained by the Trinity Centre for High Performance Computing. This cluster was funded through grants from Science Foundation Ireland. Finally, we would like to acknowledge the anonymous reviewers for their comments on the previous and current versions of the article. *Conflict of Interest*: None declared.

References

Agosta F, Valsasina P, Absinta M, Riva N, Sala S, Prelle A, Copetti M, Comola M, Comi G, Filippi M. 2011. Sensorimotor functional connectivity changes in amyotrophic lateral sclerosis. Cereb Cortex. 21:2291–2298.

Al-Chalabi A, Hardiman O. 2013. The epidemiology of ALS: a conspiracy of genes, environment and time. Nat Rev Neurol. 9:617–628.

Al-Chalabi A, Hardiman O, Kiernan MC, Chiò A, Rix-Brooks B, van den Berg LH. 2016. Amyotrophic lateral sclerosis: moving towards a new classification system. Lancet Neurol. 15: 1182–1194.

Bede P, Bokde AL, Byrne S, Elamin M, McLaughlin RL, Kenna K, Fagan AJ, Pender N, Bradley DG, Hardiman O. 2013. Multiparametric MRI study of ALS stratified for the C9orf72 genotype. Neurology. 81:361–369.

Bede P, Hardiman O. 2014. Lessons of ALS imaging: pitfalls and future directions—a critical review. Neuroimage Clin. 4:436–443.

Bede P, Iyer PM, Schuster C, Elamin M, Mclaughlin RL, Kenna K, Hardiman O. 2016. The selective anatomical vulnerability of ALS: 'disease-defining' and 'disease-defying' brain regions. Amyotroph Lateral Scler Frontotemporal Degener. 17:561–570.

Benjamini Y, Hochberg Y. 1995. Controlling the false discovery rate: a practical and powerful approach to multiple testing. J R Stat Soc Ser B Methodol. 57:289–300.

Benjamini Y, Krieger AM, Yekutieli D. 2006. Adaptive linear step-up procedures that control the false discovery rate. Biometrika. 93:491–507.

Blain-Moraes S, Mashour GA, Lee H, Huggins JE, Lee U. 2013. Altered cortical communication in amyotrophic lateral sclerosis. Neurosci Lett. 543:172–176.

Burke T, Pinto-Grau M, Lonergan K, Bede P, O'Sullivan M, Heverin M, Vajda A, McLaughlin RL, Pender N, Hardiman O. 2017. A cross-sectional population-based investigation into behavioral change in amyotrophic lateral sclerosis: subphenotypes, staging, cognitive predictors, and survival. Ann Clin Transl Neurol. 4:305–317.

Byrne S, Elamin M, Bede P, Hardiman O. 2012. Absence of consensus in diagnostic criteria for familial neurodegenerative diseases. J Neurol Neurosurg Psychiatry. 83:365–367.

Byrne S, Heverin M, Elamin M, Bede P, Lynch C, Kenna K, MacLaughlin R, Walsh C, Al Chalabi A, Hardiman O. 2013. Aggregation of neurologic and neuropsychiatric disease in amyotrophic lateral sclerosis kindreds: a population-based case–control cohort study of familial and sporadic amyotrophic lateral sclerosis. Ann Neurol. 74:699–708.

Cedarbaum JM, Stambler N, Malta E, Fuller C, Hilt D, Thurmond B, Nakanishi A. 1999. The ALSFRS-R: a revised ALS functional rating scale that incorporates assessments of respiratory function. J Neurol Sci. 169:13–21.

de Carvalho M, Chio A, Dengler R, Hecht M, Weber M, Swash M. 2005. Neurophysiological measures in amyotrophic lateral sclerosis: markers of progression in clinical trials. Amyotroph Lateral Scler. 6:17–28.

de Carvalho M, Swash M. 2016. Lower motor neuron dysfunction in ALS. Clin Neurophysiol. 127:2670–2681.

Destrieux C, Fischl B, Dale A, Halgren E. 2010. Automatic parcellation of human cortical gyri and sulci using standard anatomical nomenclature. Neuroimage. 53:1–15.

Dukic S, Iyer PM, Mohr K, Hardiman O, Lalor EC, Nasseroleslami B 2017. Estimation of coherence using the median is robust against EEG artefacts. In: 2017 39th Annual International Conference of the IEEE Engineering in Medicine and Biology Society (EMBC). Presented at the 2017 39th Annual International Conference of the IEEE Engineering in Medicine and Biology Society (EMBC). pp. 3949–3952.

Efron B. 2007. Size, power and false discovery rates. Ann Stat. 35:1351–1377.

Efron B, Tibshirani R, Storey JD, Tusher V. 2001. Empirical Bayes analysis of a microarray experiment. J Am Stat Assoc. 96: 1151–1160.

Eklund A, Nichols TE, Knutsson H. 2016. Cluster failure: why fMRI inferences for spatial extent have inflated false-positive rates. Proc Natl Acad Sci USA. 113:7900–7905.

Elamin M, Pinto-Grau M, Burke T, Bede P, Rooney J, O'Sullivan M, Lonergan K, Kirby E, Quinlan E, Breen N, et al. 2017.

Identifying behavioural changes in ALS: validation of the Beaumont Behavioural Inventory (BBI). Amyotroph Lateral Scler Frontotemporal Degener. 18:68–73.

Fisher KM, Zaaimi B, Williams TL, Baker SN, Baker MR. 2012. Beta-band intermuscular coherence: a novel biomarker of upper motor neuron dysfunction in motor neuron disease. Brain. 135:2849–2864.

Fukunaga K. 1990. Introduction to statistical pattern recognition. 2nd ed. San Diego, CA, USA: Morgan Kaufmann.

Georgopoulos AP, Karageorgiou E, Leuthold AC, Lewis SM, Lynch JK, Alonso AA, Aslam Z, Carpenter AF, Georgopoulos A, Hemmy LS, et al. 2007. Synchronous neural interactions assessed by magnetoencephalography: a functional biomarker for brain disorders. J Neural Eng. 4:349.

Halliday DM, Rosenberg JR, Amjad AM, Breeze P, Conway BA, Farmer SF. 1995. A framework for the analysis of mixed time series/point process data—theory and application to the study of physiological tremor, single motor unit discharges and electromyograms. Prog Biophys Mol Biol. 64:237–278.

Hardiman O, van den Berg LH, Kiernan MC. 2011. Clinical diagnosis and management of amyotrophic lateral sclerosis. Nat Rev Neurol. 7:639–649.

Herman P, Prasad G, McGinnity TM, Coyle D. 2008. Comparative analysis of spectral approaches to feature extraction for EEG-based motor imagery classification. IEEE Trans Neural Syst Rehabil Eng. 16:317–326.

Huynh W, Simon NG, Grosskreutz J, Turner MR, Vucic S, Kiernan MC. 2016. Assessment of the upper motor neuron in amyotrophic lateral sclerosis. Clin Neurophysiol. 127: 2643–2660.

Iyer PM, Egan C, Pinto-Grau M, Burke T, Elamin M, Nasseroleslami B, Pender N, Lalor EC, Hardiman O. 2015. Functional connectivity changes in resting-state EEG as potential biomarker for amyotrophic lateral sclerosis. PLoS One. 10:e0128682.

Iyer PM, Mohr K, Broderick M, Gavin B, Burke T, Bede P, Pinto-Grau M, Pender NP, McLaughlin R, Vajda A, et al. 2017. Mismatch negativity as an indicator of cognitive subdomain dysfunction in amyotrophic lateral sclerosis. Front Neurol. 8:395/1–395/11.

Izenman AJ. 2008. Modern multivariate statistical techniques: regression, classification, and manifold learning, springer texts in statistics. New York, NY, USA: Springer.

Jolliffe IT. 2002. Principal component analysis. 2nd ed. New York, NY, USA: Springer.

Khan S, Michmizos K, Tommerdahl M, Ganesan S, Kitzbichler MG, Zetino M, Garel K-LA, Herbert MR, Hämäläinen MS, Kenet T. 2015. Somatosensory cortex functional connectivity abnormalities in autism show opposite trends, depending on direction and spatial scale. Brain. 138:1394–1409.

Kiernan MC, Vucic S, Cheah BC, Turner MR, Eisen A, Hardiman O, Burrell JR, Zoing MC. 2011. Amyotrophic lateral sclerosis. Lancet. 377:942–955.

Langheim FJP, Leuthold AC, Georgopoulos AP. 2006. Synchronous dynamic brain networks revealed by magnetoencephalography. Proc Natl Acad Sci USA. 103:455–459.

Lei X, Wu T, Valdes-Sosa PA. 2015. Incorporating priors for EEG source imaging and connectivity analysis. Front Neurosci. 9: 284.

Leonardi N, Richiardi J, Gschwind M, Simioni S, Annoni J-M, Schluep M, Vuilleumier P, Van De Ville D. 2013. Principal components of functional connectivity: a new approach to study dynamic brain connectivity during rest. Neuroimage. 83:937–950.

Mohr K, Nasseroleslami B, Iyer PM, Hardiman O, Lalor EC 2017. EyeBallGUI: A Tool for Visual Inspection and Binary Marking of Multi-Channel Bio-Signals. bioRxiv. 129437.

Muthukumaraswamy SD. 2013. High-frequency brain activity and muscle artifacts in MEG/EEG: a review and recommendations. Front Hum Neurosci. 7:138.

Muthuraman M, Hellriegel H, Hoogenboom N, Anwar AR, Mideksa KG, Krause H, Schnitzler A, Deuschl G, Raethjen J. 2014. Beamformer source analysis and connectivity on concurrent EEG and MEG data during voluntary movements. PLoS One. 9:e91441.

Muthuraman M, Moliadze V, Mideksa KG, Anwar AR, Stephani U, Deuschl G, Freitag CM, Siniatchkin M. 2015. EEG-MEG integration enhances the characterization of functional and effective connectivity in the resting state network. PLoS One. 10:e0140832.

Nasseroleslami B, Lakany H, Conway BA 2011. Identification of time-frequency EEG features modulated by force direction in arm isometric exertions. In: 2011 5th International IEEE/EMBS Conference on Neural Engineering (NER). Presented at the 2011 5th International IEEE/EMBS Conference on Neural Engineering (NER). pp. 422–425.

Nasseroleslami B, Lakany H, Conway BA. 2014. EEG signatures of arm isometric exertions in preparation, planning and execution. Neuroimage. 90:1–14.

Nolan H, Whelan R, Reilly RB. 2010. FASTER: fully automated statistical thresholding for EEG artifact rejection. J Neurosci Methods. 192:152–162.

Oishi K, Zilles K, Amunts K, Faria A, Jiang H, Li X, Akhter K, Hua K, Woods R, Toga AW, et al. 2008. Human brain white matter atlas: identification and assignment of common anatomical structures in superficial white matter. Neuroimage. 43: 447–457.

Pfurtscheller G, Lopes da Silva FH. 1999. Event-related EEG/MEG synchronization and desynchronization: basic principles. Clin Neurophysiol. 110:1842–1857.

Pievani M, de Haan W, Wu T, Seeley WW, Frisoni GB. 2011. Functional network disruption in the degenerative dementias. Lancet Neurol. 10:829–843.

Ramírez RR, Wipf D, Baillet S. 2010. Neuroelectromagnetic source imaging of brain dynamics. In: Chaovalitwongse W, Pardalos PM, Xanthopoulos P, editors. Computational Neuroscience. New York, NY: Springer New York. p. 127–155.

Rascovsky K, Hodges JR, Knopman D, Mendez MF, Kramer JH, Neuhaus J, van Swieten JC, Seelaar H, Dopper EGP, Onyike CU, et al. 2011. Sensitivity of revised diagnostic criteria for the behavioural variant of frontotemporal dementia. Brain. 134:2456–2477.

Schuster C, Elamin M, Hardiman O, Bede P. 2016. The segmental diffusivity profile of amyotrophic lateral sclerosis associated white matter degeneration. Eur J Neurol. 23:1361–1371.

Stam CJ, Jones BF, Manshanden I, van Cappellen van Walsum AM, Montez T, Verbunt JPA, de Munck JC, van Dijk BW, Berendse HW, Scheltens P. 2006. Magnetoencephalographic evaluation of resting-state functional connectivity in Alzheimer's disease. Neuroimage. 32:1335–1344.

Stoffers D, Bosboom JLW, Deijen JB, Wolters EC, Stam CJ, Berendse HW. 2008. Increased cortico-cortical functional connectivity in early-stage Parkinson's disease: An MEG study. Neuroimage. 41:212–222.

Turner MR, Kiernan MC. 2012. Does interneuronal dysfunction contribute to neurodegeneration in amyotrophic lateral sclerosis? Amyotroph Lateral Scler. 13:245–250.

Vecchio F, Babiloni C, Lizio R, Fallani FV, Blinowska K, Verrienti G, Frisoni G, Rossini PM. 2012. Resting state cortical EEG rhythms in Alzheimer's disease: toward EEG markers for clinical applications: a review. Suppl Clin Neurophysiol. 62: 223–236.

Vuckovic A, Hasan MA, Fraser M, Conway BA, Nasseroleslami B, Allan DB. 2014. Dynamic oscillatory signatures of central neuropathic pain in spinal cord injury. J Pain. 15: 645–655.

Vuckovic A, Hasan MA, Osuagwu B, Fraser M, Allan DB, Conway BA, Nasseroleslami B. 2015. The influence of central neuropathic pain in paraplegic patients on performance of a motor imagery based Brain Computer Interface. Clin Neurophysiol. 126:2170–2180.

Xu R, JIANG N, Vuckovic A, Hasan M, Mrachacz-Kersting N, Allan D, Fraser M, Nasseroleslami B, Conway B, Dremstrup K, et al. 2014. Movement-related cortical potentials in paraplegic patients: abnormal patterns and considerations for BCI-rehabilitation. Front Neuroeng. 7:35.

Zhou X-H, McClish DK, Obuchowski NA. 2009. Statistical methods in diagnostic medicine. Hoboken, NJ, USA: John Wiley & Sons.